KAGUYA SELENODESY AND THE SOUTH POLE-AITKEN BASIN. S. Sasaki[1], S. Goossens[1#], Y. Ishihara[1], H. Araki[1], H. Hanada[1], K. Matsumoto[1], H. Noda[1], F. Kikuchi[1], T. Iwata[2]. [1]RISE Project, National Astronomical Observatory of Japan, 2-12 Hoshigaoka, Mizusawa, Oshu 023-0861 Japan (sho@miz.nao.ac.jp), [2] ISAS/JAXA, Sagamihara, Japan, #Now at Goddard Space Flight Center/NASA, USA.

Introduction: The Japanese lunar explorer KAGUYA (SELENE) was launched on September 14th, 2007 by JAXA and ended its operation on June 10th, 2009. From polar orbits with 100km average altitude, KAGUYA observed the global Moon by June 10, 2009. Among 14 instruments on board KAGUYA, there are two subsatellites Rstar (OKINA) and Vstar (OUNA). KAGUYA obtained first global topography and gravity of the Moon. Moreover, the laser altimeter (LALT) on board KAGUYA obtained the first precise global topography of the Moon with range accuracy of 5m [1]. Range data exceeded 20 million points.

Synchronous rotation of the Moon with its orbit inhibits a direct link between a ground tracking station on the Earth and a lunar-orbiting spacecraft over the farside. KAGUYA has two small spin-stabilized subsatellites, Rstar (OKINA) and Vstar (OUNA) for gravity measurement. We tracked the three satellites by new methods: 4-way Doppler tracking between the ground station and the main satellite via Rstar for the farside gravity and multi-frequency differential VLBI tracking between Rstar and Vstar. Precise determination of Rstar orbit by VLBI is important for the gravity measurement through the 4-way tracking of the main satellite. The global lunar gravity field with unprecedented accuracy was obtained. KAGUYA obtained accurate lunar farside gravity for the first time [2].

From one-year tracking data, lunar gravity field model SGM100h was obtained [3] and the model was refined into SGM100i taking into account VLBI data [4]. The latest version of gravity data is SGM150j [5]. The gravity and topography data have been processed mainly at National Astronomical Observatory of Japan. KAGUYA selenodesy data are opened to public through the site: http://www.miz.nao.ac.jp/rise-pub/en .

Bouguer gravity anomaly, Moho depth, and crustal thickness are obtained [6], using crustal density 2800 kg/m^3, mantle density 3360 kg/m^3, assuming uniform crustal density. The crustal thickness was constrained on the basis that the minimum thickness is not negative. The crustal thickness is nearly zero benearth Mare Moscoviense [6], which would have been formed by multiple impacts and resulting strong mantle uplift [7].

South Pole Aitken Basin: The South Pole-Aitken basin (hereafter SPA) is the largest (2400km in diameter), deepest and presumably oldest impact basin in the solar system. SPA has a degraded morphology and abundant superimposed craters. From the topography and the crustal thickness by KAGUYA, the proposed elliptic shape of SPA [8] was confirmed.

To see detailed structure, we use localized representation of gravity potential [9] where Slepian functions were used to estimate the gravity field over certain areas of the Moon. We express the gravitational potential with localized spherical harmonics functions [10]. We include data in a spherical cap area with a radius of 40 degree from the SPA center. This area is fully covered by 4-way Doppler tracking of the KAGUYA main satellite. We obtained gravity adjustment between plus and minus 68 mGal with an RMS of 17 mGal [10]. The revised gravity field improved data of crustal thickness with slightly higher resolutions.

The region with the thinnest crust is offset southward from the center of SPA, where Moho depth at the central region of SPA is around 30km (25km in crustal thickness). The offset could be ascribed to the oblique impact hypothesis [8].

Note that the crustal thickness is affected by the assumed anorthosite crustal density 2800 kg/m^3. KAGUYA MI showed evidence of anorthosite in SPA [11] but outside the central region. Spectral data of central peaks of craters inside the central region of SPA show ultramafic assemblage dominated by Magnesium rich orthopyroxene, probably composed of impact melt sheet [12]. Then, higher crustal density would result in larger crustal thickness (30-35km). The presence of lower crust in SPA was suggested by previous gravity analysis [13].

Since Bouguer anomaly is relatively flat inside SPA as well as in the farside highland [3], surface morphologies could be supported by elastically in SPA. However, there are overprinted small impact basins with gravity anomaly. We analyzed structure of small basins in and around SPA (Fig. 1 and Table). We interpret that a positive gravity anomaly at the basin corresponds to a Moho uplift (Fig. 2 and Table).

Apollo basin has a distinct gravity anomaly with the thinnest crust (shallowest Moho) (Fig.2). This would correspond to a large mantle plug. Just around the rim of SPA adjacent Schrödinger basin, obscure circular structure Amundsen-Ganswindt has a distinct Moho uplift, suggesting a buried impact structure. A distinct Moho uplift beneath Schrödinger corresponds to the presence of olivine at the central peak rings there [14]. Ingeni and Zeeman also have olivine signature and they are associated with Moho undulation. Between adjacent Poincaré and Planck, older, less distinct Poincaré shows stronger gravity anomaly/Moho uplift. The observed anomaly corresponds to Type 2 like anomaly [2], where a significant uplift at the center is probably due to overcompensation after the impact. In general, basin structures in the central SPA show little gravity anomaly. Although it might be due to lower spatial resolution, there are several possibilities such as less density difference between crust and mantle and rapid relaxation of the uplift. The localized analysis with higher resolution found Moho undulation at Zeeman.

References: [1] Araki, H. et al., (2009) Science 323, 897, [2] Namiki, N. et al. (2009) Science, 323, 900, [3] Matsumoto, K. et al. (2010) JGR 115, E06007, [4] Goossens, S. et al. (2010), J. Geodesy, 85, 205-228.[5] Goossens et al.(2011) AGU Fall Meeting, P44B-05, [6] Ishihara, Y. et al. (2009) GRL, 36, L19202, [7] Ishihara, Y. et al. (2011) GRL, 38, L03201, [8] Garrick-Bethell & Zuber (2009) Icarus 204, 399, [9] Han, S.-C. (2008) JGR 113, E11012, [10] Goossens, S. et al. (2012) JGR, in press, [11] Ohtake, M. et al. (2009) Nature 461, 237, [12] Nakamura, R. et al. (2009) GRL 36, L22202, [13] Wieczorek, M. A., Phillips, R. J. (1999) Icarus 139, 246, [14] Yamamoto, S. et al. (2010) Nature Geoscience 3, 533.

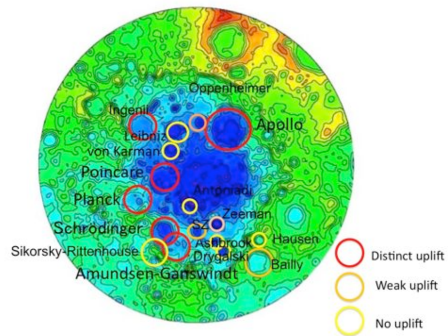

Fig. 1. Impact basins in SPA overprinted on the topography map.

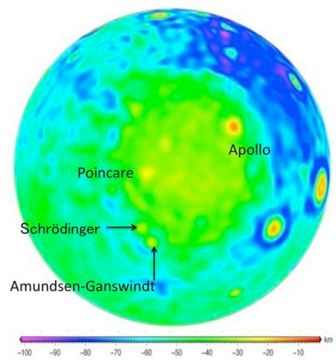

Fig. 2. Moho depth map of SPA region, indicating some basins with distinct Moho uplift.

Table 1 Impact basins in SPA regions.

			Diameter[km]	Clarity	Mare	Moho Uplift	Crustal Thickness	Age
Apollo	36.1S	151.8W	538	Y	Y	Y	7	Pre-Nec(9)
Amundsen -Ganswindt	81S	120E	335	N	N	Y	26	Pre-Nec(7)
Poincaré	56.7S	163.6E	319	Y	Y	Y	13	Pre-Nec(4)
Ingenii	33.7S	163.5E	315-660	Y	Y	Y	25	Pre-Nec(4)
Planck	57.9S	136.8E	314	Y	N	Y	33	Pre-Nec(7)
Schrödinger	75S	132.4E	312	Y	Y	Y	22	Imbrian(12)
Sikorsky -Rittenhouse	68S	111E	310	N	N	N	48	Nectarian(11)
Bailly	66.5S	69.1W	300	Y	N	P	47	Nectarian(11)
Schrödinger -Zeeman	81S	165W	250	N	N	P	28	
Leibnitz	38.3S	179.2E	245	Y	Y	N	25	Pre-Nec
Oppenheimer	35.2S	166.3W	208	Y	Y	P	23	
Zeeman	75.2S	133.6W	190	Y	N	P#	31	
Von Kármán	44.8S	175.9E	180	Y	Y	N	21	Pre-Nec
Hausen	65.0S	88.1W	167	Y	N	N	60	
Ashbrook	81.4S	112.5W	156	Y	N	N	39	
Drygalski	79.3S	84.9W	149	Y	N	N	45	
Antoniadi	69.7S	172W	143	Y	Y	N	25	Imbrian(12)

Y: Yes, N: No, P: Probable # Around Zeeman, distinct Moho undulation is observed by high-resolution map.